Research Report

96-27

Application of the Matrix Converter to Induction Motor Drives

T. Matsuo, S. Bernet, R.S. Colby*, T.A. Lipo

Wisconsin Power Electronics
Research Center
University of Wisconsin-Madison
Madison WI 53706-1691

*Otis Elevator Company
5 Farm Springs Rd
Farmington CT 06032

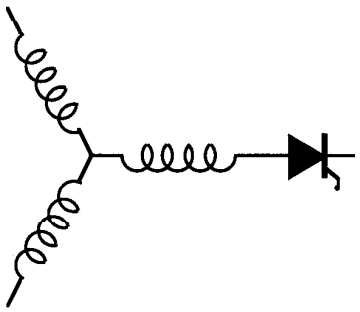

Wisconsin
Electric
Machines &
Power
Electronics
Consortium

University of Wisconsin-Madison
College of Engineering
Wisconsin Power Electronics Research Center
2559D Engineering Hall
1415 Engineering Drive
Madison WI 53706-1691

Application of the Matrix Converter to Induction Motor Drives

Takayoshi Matsuo, Steffen Bernet, R. Stephen Colby* and Thomas A. Lipo

University of Wisconsin-Madison
Electrical and Computer Engineering
1415 Johnson Drive
Madison, Wisconsin 53706
U. S. A.

*Otis Elevator Company
Five Farm Springs
Farmington, Connecticut 06032
U. S. A.

Abstract–This paper presents the technical issues of applying the matrix converter to field oriented induction motor drives. A newly developed matrix converter switching sequence combination is described in detail, the purpose of which is to minimize harmonic components of the matrix converter input currents. It is demonstrated that small size capacitors work efficiently as input filters. Matrix converter losses are calculated with a developed power converter loss calculation model. The calculation results indicate that the matrix converter realizes a good converter efficiency.

I. INTRODUCTION

Matrix converters are, as yet, in the realm of the research lab. However, their simple topology, absence of large dc link filter and easy control of input power factor make this circuit an attractive one. The ac to ac matrix converter was first investigated by Gyugyi and Pelly in 1976 [1]. More recently Venturini and Alesina have introduced a matrix converter design using a generalized high frequency switching strategy [2]. The matrix converter has recently attracted numerous researchers because of its advantages over the conventional dc link inverters.

The purpose of this paper is to examine in detail the technical issues of applying the matrix converter to field oriented induction motor drives. The important issues addressed in this paper are bi-directional switch configurations for implementing a matrix converter, the total silicon requirement for a 4-quadrant drive, an implementation of field oriented control with a matrix converter, filter requirements and input current characteristics, and a loss estimation of the matrix converter.

The harmonic analysis of the matrix converter input current, the filter current, and the input power source current were performed to develop a switching sequence combination which minimizes the harmonic contents of the matrix converter input current and to study the filter size. It is demonstrated that small size capacitors work efficiently as input filters to keep the input voltage from changing significantly during each PWM cycle and to prevent unwanted harmonic currents from flowing into ac main supplies.

A precise loss calculation model for power converters is described and applied to the drive system to study the loss characteristics of the matrix converter. The loss model contains besides an analytical description of the significant losses especially a new powerful algorithm which allows the determination of the occurring type of a commutation at each switching event and the distribution of the losses to the active semiconductors of a switch. Calculated converter loss and efficiency show that the matrix converter is able to realize good converter efficiency.

II MATRIX CONVERTER/INDUCTION MOTOR DRIVE

A three phase to three phase, ac to ac matrix converter basically consists of a 3 x 3 switch matrix. The 9 bi-directional voltage blocking, current conducting switches are arranged so that any input phase can be connected to any output phase at any time. The 3 x 3 switch matrix can be arranged in the form of Fig. 1 for purpose of analysis. Since an inductive load is assumed, the voltage sources of the input must be created by placing capacitors (filter) from line to line across the converter input phases. Figure 1 also includes the impedance of the main power source, that is, the leakage inductance l_s and the resistance r. In principle, for a given set of input three phase voltages, any desired set of output voltages can then be synthesized by suitably toggling the matrix switches.

Figure 1 also shows how a back to back arrangement of IGBTs may be used to implement the required bi-directional switch. The two diodes are used to provide the reverse voltage blocking capability. The diodes are also effectively placed in parallel with the IGBT by use of the short at the mid point of the two branches. The total number of sets of an IGBT and a diode that are required to implement the matrix converter of Fig. 1 is 18. This arrangement is preferable to the analogous configurations without a short at the mid point as they prevent a possible avalanche breakdown of the IGBTs during the interruption of the reverse current. Furthermore, because the common collector arrangement requires the minimum number of isolated gate drives, that is six, this switch configuration is the cheapest and also technically preferable implementation of all back-to-back configurations on the basis of conventional IGBTs. A comparison of the number of the required semiconductors shows that the matrix converter needs 6 IGBTs and 6 diodes more than the comparable PWM dc-voltage-link converter if the configuration shown in Fig. 1 is used. In spite of the

different numbers of required semiconductors, a detailed investigation of the switch ratings reported in this paper demonstrates that the installed total switch power of both circuits is generally the same due to the possible reduction of the current ratings of the switches in the matrix converter by one third.

The expense of semiconductors can be reduced even more if one uses the capability of NPT-IGBTs to block both forward and reverse voltages [5]. The elimination of the series diodes and the possible reduction of the current ratings of the IGBTs could significantly reduce the installed total switch power of the matrix converter compared to that of the dc voltage link converter.

Figure 2 shows a drive configuration for a field oriented control of an induction motor which is driven by a three phase to three phase matrix converter. By means of an incremental encoder or resolver, the angular position of the rotor θ_r is established. The angular position of the slip θ_s, which is calculated in the field oriented control module, is added to the angular position of the rotor θ_r to form the angular position of the stator MMF θ_e. These sinusoidal components are used to refer those physical stator currents from the physical (stationary) reference frame to the synchronously rotating (d-q) axes. The encoder is also used to measure speed. The voltage command signals from the field oriented controller are fed into the matrix converter block, where the matrix converter generates three phase PWM voltage pulses to drive the induction motor.

The three phase to three phase matrix converter is completed by filters at the input side. The output side filters can generally be omitted in motor drive applications, where the stator winding inductances of the motor work as the filters. One important role of the filters at input side is to keep the input voltage from changing significantly during each PWM cycle. Another important role is to absorb harmonic currents, which are generated by matrix converters, to prevent unwanted harmonic currents from flowing into ac main supplies and to satisfy any power quality regulation

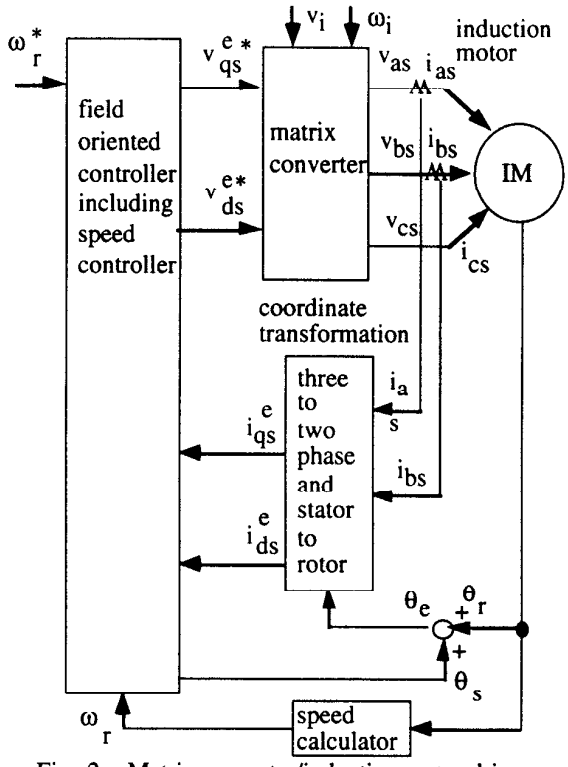

Fig. 2 Matrix converter/induction motor drive.

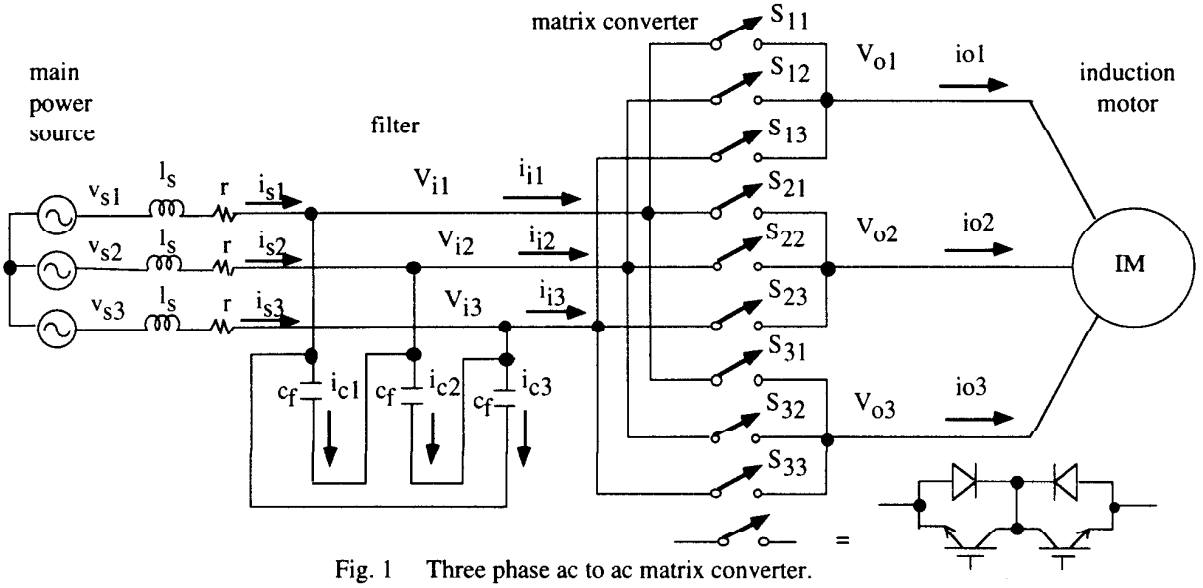

Fig. 1 Three phase ac to ac matrix converter.

applicable. A simple filter configuration was examined, as shown in Fig. 1, where a capacitor is connected between each line to line at the matrix converter input.

III. MATRIX CONVERTER MODULATION STRATEGY

Assuming that the voltages of the input are essentially constant during the switching interval, the average output voltage can be found during any switching interval by employing a modulation strategy [M(t)], which can be written in the matrix form such that [3]

$$[M(t)] \cdot [V_I(t)] = [V_O] \tag{1}$$

which is

$$\begin{bmatrix} m_{11}(t) & m_{12}(t) & m_{13}(t) \\ m_{21}(t) & m_{22}(t) & m_{23}(t) \\ m_{31}(t) & m_{32}(t) & m_{33}(t) \end{bmatrix} \cdot \begin{bmatrix} V_{i1} \\ V_{i2} \\ V_{i3} \end{bmatrix} = \begin{bmatrix} V_{o1} \\ V_{o2} \\ V_{o3} \end{bmatrix} \tag{2}$$

where

$$V_{iN} = V_I \cos(\omega_i t - (N-1)\, 2\pi/3) \tag{2}$$

$$V_{oN} = V_O \cos(\omega_o t + \theta_o - (N-1)\, 2\pi/3) + \frac{V_O}{2\sqrt{3}} \cos(3\omega_i t) - \frac{V_O}{6} \cos(3\omega_o t + 3\theta_o) \tag{3}$$

$N = 1, 2,$ and 3

where θ_o = arbitrary output voltage phase angle and T_s denotes the switching interval in seconds.

The switching periods $t_{ij}(t)$ are given by the equation

$$[T_{sw}(t)] = \begin{bmatrix} t_{11}(t)\, t_{12}(t)\, t_{13}(t) \\ t_{21}(t)\, t_{22}(t)\, t_{23}(t) \\ t_{31}(t)\, t_{32}(t)\, t_{33}(t) \end{bmatrix} = T_s\, [M(t)] \tag{4}$$

where

$$t_{i1} + t_{i2} + t_{i3} = T_s \tag{5}$$

$i = 1, 2,$ and 3

It should be noted that regardless of the switching strategy adopted, there are, however, physical limits on the output voltage achievable with this system. For complete control of the output voltage at any time, the envelope of the target output voltages must be wholly contained within the continuous envelope of the input voltages. This limit can be improved by adding a third harmonic at the input frequency to all target voltages [4]. The addition of this third harmonic increases the available output voltage range to 0.75 of the input when the third harmonic has a peak value of $V_I/4$. Further improvement of the transfer ratio can be achieved by subtracting a third harmonic at the output frequency from all target output voltages to minimize the range of the output voltage envelope to 0.866 of the peak phase voltage which allows an absolute maximum transfer ratio of 0.75/0.866 = 0.866 of V_I when this third harmonic has a peak value of $V_O/6$. Hence the maximum possible voltage transfer ratio with the modulation strategy of Eq. 1 becomes V_O/V_I = 0.75/0.866 = 0.866.

IV. SIMULATION STUDY

The implementation of the entire matrix converter/induction motor drive system into a simulation program is described in Ref. 6, which includes a three phase ac to ac matrix converter, an induction motor [4], a field oriented controller and a filter and a power source.

To illustrate how the matrix converter/induction motor drive system works, a simulation was carried out with the input source line to line voltage of 480 V rms. The filter capacitance of 10 μF and the induction motor rating of 40 kW was used for this simulation run. A waveform of the phase a motor current and a filtered waveform of the phase a matrix converter output voltage are shown in Fig. 3. Figure 4 shows a filtered waveform of the phase a matrix converter output voltage, where it is clearly shown that the matrix converter output voltage includes third harmonic components at both the input frequency and output frequency in addition to the fundamental component. Both third harmonic components do not appear on the line to line motor voltages because each matrix converter three phase output voltage has the same third harmonic component. The wave form of v_{o1} in Fig. 4 is a filtered waveform of v_{o1} in Fig. 3.

Figure 5 shows how the capacitors at the matrix converter input function as filters. Most of the harmonic components of the matrix converter input currents are absorbed into the filter capacitors. The voltage and current waveforms of the input main power source are shown also in Fig. 5, where it is demonstrated that the input power factor is controlled at near unity value. It is a practical manner to control the input power factor of the matrix converter to unity by providing the required lagging current from the matrix converter to cancel the leading current due to the filters.

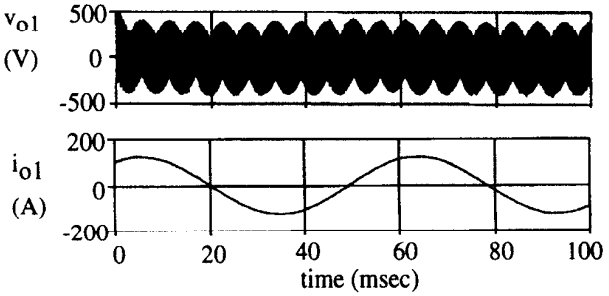

Fig. 3 Waveform of the phase a motor current and a waveform of the phase a matrix converter output voltage showing added third harmonic components at both the input and output frequencies.

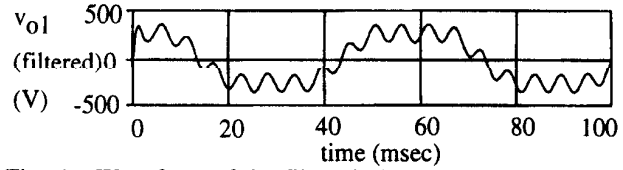

Fig. 4 Waveform of the filtered phase a matrix converter output voltage.

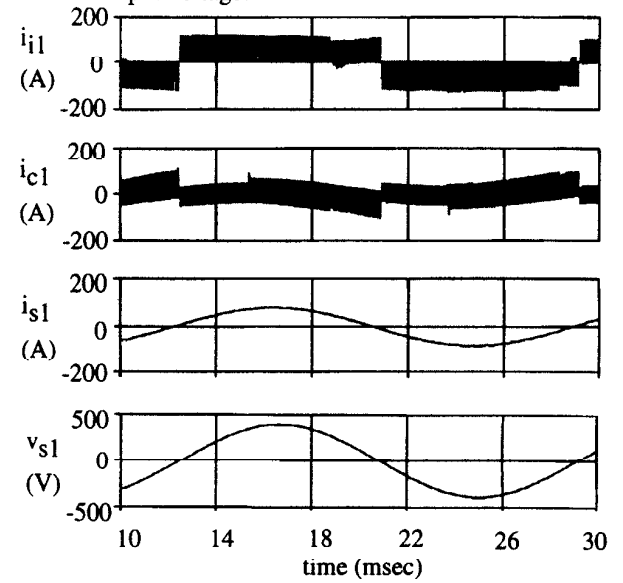

Fig. 5 Waveforms of the matrix converter input current, the filter capacitor current, the input current of the main power source and the input voltage and current of the main power source.

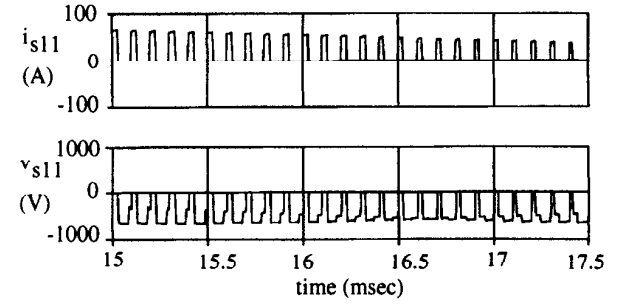

Fig. 6 Waveforms of the switch voltage and current, which is connected between the input phase 1 and the output phase 1.

The switching frequency of the matrix converter was set at 10 kHz, that is, the sampling interval of 100 μsec. The integration cycle in the ACSL program was set to carry out every 1 μsec. Typical waveforms of the voltage across one bi-directional switch and the switch current are presented in Fig. 6.

V. SWITCHING STRATEGY AND HARMONIC CURRENT ANALYSIS

Harmonic components of the matrix converter input currents, filter capacitor currents, and input source currents were analyzed to determine the size of the filter. Harmonic analyses were also utilized to develop a switching strategy [5] which reduces harmonics in the matrix converter input currents.

Each output phase of a three phase to three phase matrix converter is connected to each three input phase for a certain time period during each switching interval. Each time period is determined so that each output voltage is to be an average voltage of three input voltage pulses.

$$v_{01} = v_{i1} * \frac{t_{11}}{T_s} + v_{i2} * \frac{t_{12}}{T_s} + v_{i3} * \frac{t_{13}}{T_s} \quad (6)$$

$$v_{02} = v_{i1} * \frac{t_{21}}{T_s} + v_{i2} * \frac{t_{22}}{T_s} + v_{i3} * \frac{t_{23}}{T_s} \quad (7)$$

$$v_{03} = v_{i1} * \frac{t_{31}}{T_s} + v_{i2} * \frac{t_{32}}{T_s} + v_{i3} * \frac{t_{33}}{T_s} \quad (8)$$

The input phase 1 voltage appears in output phase 1 for a time interval t_{11}, the input phase 2 voltage for a time interval t_{12}, and the input phase 3 voltage for a time interval t_{13}, where $t_{11} + t_{12} + t_{13} = T_s$ and the switching interval $T_s = 1/f_s$ (f_s is the switching frequency). When the switching frequency f_s is 10 kHz the switching interval T_s = 100 μsec. There is no restriction on the sequence of the three time intervals, that is, the output phase 1 can be connected to the input phase 2 first and then phase 3 and phase 1, or to the input phase 3 first and then phase 1 and phase 2. The output voltage v_{01} remains same in either switching sequence combinations. There are basically 216 different switching sequence combinations for a nine-switch three phase to three phase matrix converter to produce specific three phase output voltages. Matrix converter input current characteristics depend on the switching sequence combinations while output current characteristics are not significantly affected by the change of the switching sequence combinations.

Figure 7 illustrates a natural choice of switching sequence combination (#1 SSC), where the waveforms of the three phase output voltages and the matrix converter input currents are presented for one switching interval, that is 100 μsec. The output phase 1 (Output 1) is connected to the input phase 1 (Input 1) first, then to the input phase 2 (Input 2) next, and then to the input phase 3 (Input 3). The three phase input voltage waveforms can be found in the three phase output voltage waveforms for specific time intervals. The output phase 2 (Output 2) is connected to Input 2 first and then to Input 3 next, then to Input 1. The output phase 3 (Output 3) is connected to Input 3 first and then to Input 1 next, then to Input 2. With the #1 SSC the three phase matrix converter input currents are well balanced and the lowest major harmonic components are located near the switching frequency, which is shown in Fig. 8 of the spectrum profile of the input current.

Figure 9 illustrates another switching sequence combination (#2 SSC). Output 1 is connected to Input 1 first, then to Input 2 next, and then to Input 3, which is the same switching sequence as the #1 SSC. Output 2 is

connected to Input 1 first and then to Input 2 next, then to Input 3. Output 3 is connected to Input 1 first and then to Input 2 next, then to Input 3. As shown in Fig. 9, during the time period of t_{11} the input phase 1 is connected to all the output phases, that means that $i_{i1} = i_{o1} + i_{o2} + i_{o3} = 0$. Also $i_{i1} = 0$ during the time period of $T_s - t_{31}$ because no output phases are connected to the input phase 1. The input phase 2 current $i_{i2} = 0$ during the time periods t_{11} and t_{33} because no output phases are connected to the input phase 2. During the time period t_{33} the input phase 3 is connected to all the output phases, which means $i_{i3} = 0$, and also $i_{i3} = 0$ during the time period of $T_s - t_{13}$. With the #2 SSC, the rms values of the input currents i_{i1}, i_{i2}, and i_{i3} are 39 %, 17 %, 39 %, respectively, less than ones with the #1 SSC. While the fundamental components of the input currents are balanced with the same value as one with #1 SSC, the rms values are not balanced, which is visible when comparing the input current waveforms of Fig. 9 with ones of Fig. 7. The rms current of the input phase 2 is 34 % larger than the input phases 1 and 3. With the #2 SSC the lowest major harmonic components are found near the switching frequency.

Similar switching sequence combinations can be developed to reduce the input current harmonics. Figure 10 (a) illustrates #3 switching sequence combination (#3 SSC). All the output phases are connected to Input 2 first, then to Input 3 next, and then to Input 1. With the #3 SSC, the rms values of the input currents i_{i1}, i_{i2}, and i_{i3} are 39 %, 39 %, 17 %, respectively, less than ones with the #1 SSC, while the fundamental components of the input currents remain the same as ones with #1 or #2 SSC. Figure 10 (b) illustrates

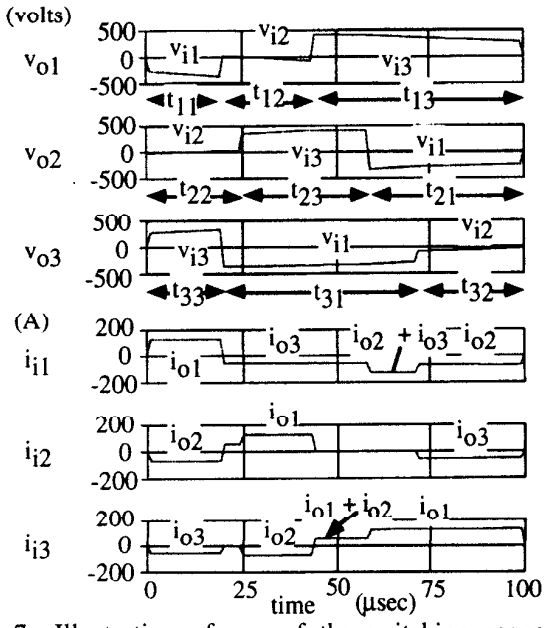

Fig. 7 Illustration of one of the switching sequence combinations (#1 SSC) showing waveforms of three phase output voltages and three phase input currents during one switching interval.

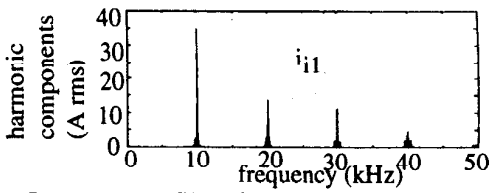

Fig. 8 Spectrum profile of the matrix converter input current with the #1 SSC.

#4 switching sequence combination (#4 SSC). All the output phases are connected to Input 3 first, then to Input 1 next, and then to Input 2. With the #3 SSC the rms values of the input currents i_{i1}, i_{i2}, and i_{i3} are 17 %, 39 %, 39 %, respectively, less than ones with the #1 SSC. With the #3 and #4 SSCs the lowest major harmonic components are found near the switching frequency.

The #2, #3 and #4 switching sequence combinations produce less harmonics at the matrix converter input though the three phase input currents are not balanced. Balanced three phase input current can be obtained by alternating the three switching sequence combinations. The switching sequence combination #5 (#5 SSC) was developed to obtain the minimum and balanced three phase input currents. The #5 SSC alternates the #2, #3 and #4 SSCs every switching interval, which is shown in Fig. 11. The three phase input currents are balanced and 31 % less than the ones with the #1 SSC. However, the #5 SSC produces harmonic currents near frequencies of every one third of the switching frequency due to the additionally introduced modulation, where the lowest major harmonic components are near 3.3 kHz. Figure 12 shows a spectrum profile of the input current i_{i1}. It is

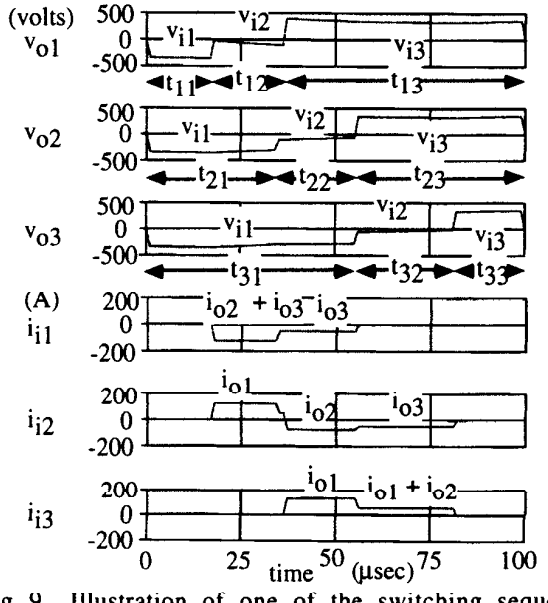

Fig. 9 Illustration of one of the switching sequence combinations (#2 SSC) showing waveforms of three phase output voltages and three phase input currents during one switching interval.

observed that the harmonic components near 3.3 kHz are amplified due to the resonance between the filter capacitance and the input source inductance and become major harmonic components of the input source current while higher frequency components of harmonic currents are well absorbed by the filters.

It is important to keep harmonic components near the switching frequency to avoid harmful harmonic amplification. To avoid the spread of harmonic current components, the switching sequence combination #6 (#6 SSC) was developed. The #6 SSC alternates the #2, #3 and #4 SSCs at a low frequency, that is, for example, applying the #2 SSC for 100 milliseconds and then the #3 SSC for next 100 milliseconds and the #4 SSC for next 100 milliseconds and repeating the sequences. Low alternating frequency keeps the lowest major harmonic components near the switching frequency. The three phase input currents are well balanced and 31 % less than the ones with the #1 SSC. Figure 13 shows the spectrum profiles of the matrix converter input current, the filter capacitor current and the input source current. The distortion index (THD) is 0.14 for the filter capacitance of 10 μF with the major harmonic components of near the switching frequency. The developed switching sequence combination #6 is an optimum switching sequence combination for the three-phase to three-phase matrix converter to obtain minimum distortion and balanced three-phase input current characteristics.

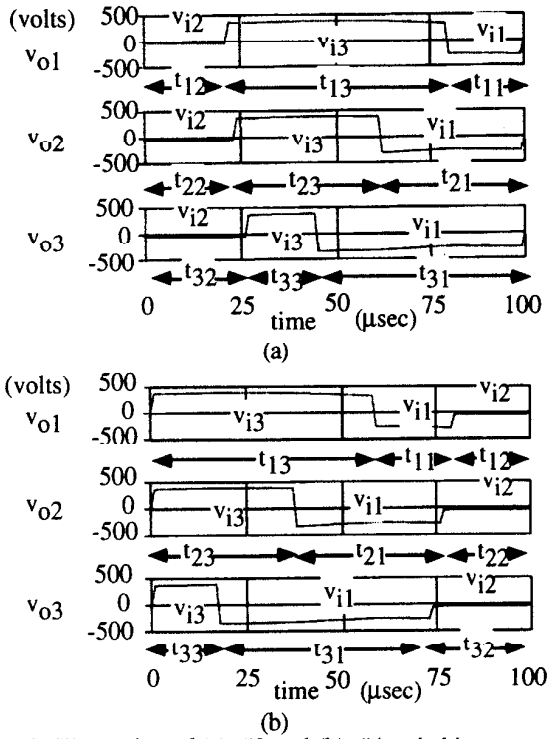

Fig. 10 Illustration of (a): #3 and (b): #4 switching sequence combinations (#3 and #4 SSC) showing waveforms of three phase output voltages and three phase input currents during one switching interval.

It is a practical manner to control the power factor of the matrix converter to cancel the leading currents provided by the filter capacitors in order to makes the input power factor of the drive system unity.

The distortion indexes are calculated for different values of the filter capacitance. With the filter capacitance of 5 μF the distortion index was 0.25 and 0.1 for the filter capacitance of 20 μF.

It is assumed for developing the control strategy of the matrix converter that the voltages at the matrix converter input are essentially constant during the switching interval and have sinusoidal waveforms of a commercial frequency of

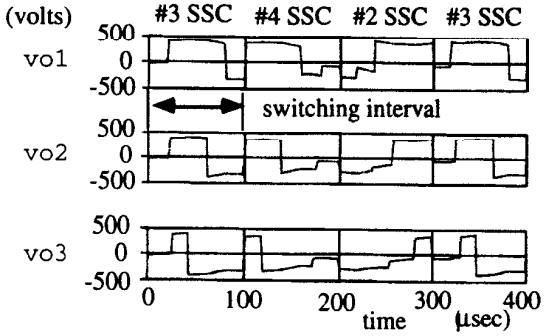

Fig. 11 Illustration of #5 switching sequence combination (#3 and #4 SSC) showing waveforms of three phase output voltages and three phase input currents during one switching interval.

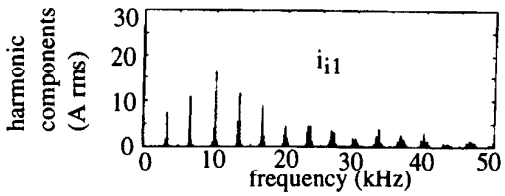

Fig. 12 Spectrum profile of the matrix converter input current with the #5 SSC.

60 Hz. However, the strategy is not correct with filter capacitance at the matrix converter input. Figure 14 shows waveforms of the three phase voltages at the matrix converter input for the case of the filter capacitance of 10 μF. The voltages are oscillates slightly due to the resonance between the filter capacitance and the source inductance.

This input voltage variations have some influence to the performance of current control of an induction motor. It was found that a proper current control response is essentially required to establish a stable induction motor current (torque) control system.

VI. SIMULATED LOSSES AND EFFICIENCY

Matrix converter losses can be calculated with a

previously developed power converter loss calculation model [6]. To guarantee a reliable operation of the matrix converter at a 480V main even at overload of the induction machine of

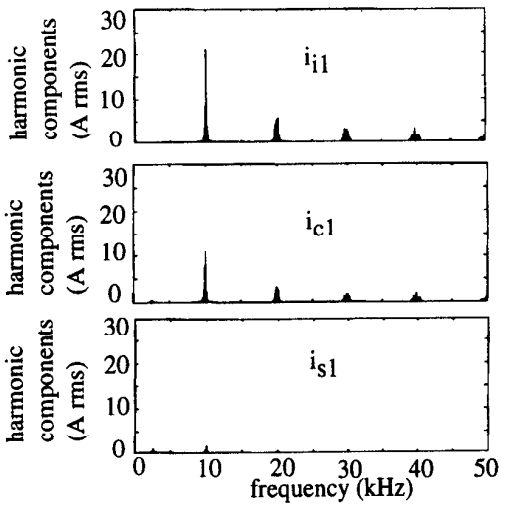

Fig. 13 Spectrum profiles of the matrix converter input current, the filter capacitor current, and the input source current with the #6 SSC in the case of the filter capacitance of 10 µF.

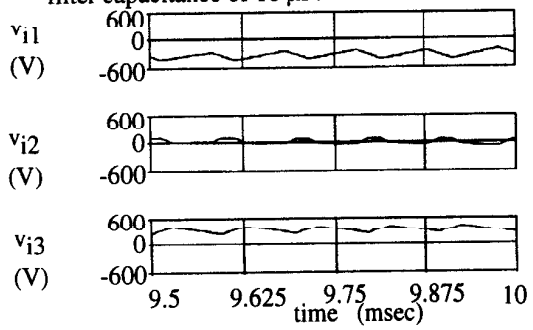

Fig. 14 Simulation results of waveforms of input voltages of a matrix converter. The filter capacitance is 5 µF. The motor speed is 100 % and the motor torque is 1 p.u.

40 kW (e.g. i_{omax}=260A) the single NPT-IGBT module SKM400GA 122D (1200V; 300A) has been chosen initially.

Figure 15 shows the computed converter losses as a function of the rated motor torque for three different speeds. Obviously the losses are strongly dependent on the torque which determines the load current. The decrease of the losses at high torques and speeds (e.g. 150% torque; 100% speed) is caused by the effective reduction of the switching frequency at the upper limit of the maximum output voltage of the converter.

Figure 16 represents the corresponding function of the converter efficiency versus the real input power of the converter. The efficiency lies in a band between 70% to 96.6% in the considered working point range. In particular, the efficiencies of 92.5% to 96.6% at medium and high speed (50%, 100%) and high torques (100%-150% rated torque) appear to be considerably higher than those of a comparable hard switching PWM rectifier/ dc-voltage-link/ inverter topology.

The dependence of the converter losses of the motor speed for two different torques in Fig. 17 shows again that the converter losses are determined completely by the motor torque if the converter does not operate near of its voltage limit where the effective switching frequency is reduced.

It can be seen in the corresponding diagram of Fig. 18 that the efficiency increases quickly if at constant torque (meaning nearly constant losses) the speed and therefore also the input power are increased.

Figure 19 represents the converter efficiency as a function of the switching frequency of the matrix converter. Because of both the hard turn on and turn off transients the converter efficiency decreases substantially with an increase of the switching frequency. The maximum permissible total power dissipation of the switches limits the maximum switching frequency to f_{smax}=30kHz even at overload (e.g. i_{omax}=260A) if the temperature of the heatsink is 80°C. However the poor converter efficiency at high switching frequencies is the reason therefore that the switching frequency of a hard switching matrix converter should generally not exceed 20kHz-25kHz.

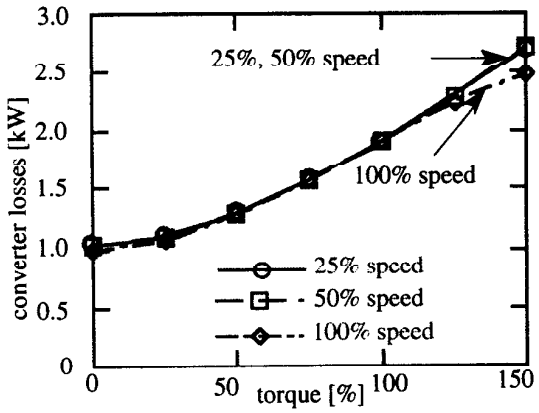

Fig. 15 Matrix converter losses versus the normalized motor torque for various speeds (SKM400GA122D; T_j=125°C; f_s=10kHz).

Detailed investigations have shown that relatively small 200A-IGBT modules (SKM300GA 122D) could be applied due to the effective parallel connection of the switches of the three switch groups. In this case the IGBT-losses limit the maximum switching frequency to f_{smax}=40kHz (i_{omax}=115A) and f_{smax}=15kHz (i_{omax}=260A) respectively. If one takes this possible reduction of the current ratings of the switches of a matrix converter into account, the total expense of semiconductors of a matrix converter is exactly the same as that of a comparable hard switching PWM rectifier/dc-voltage-link/inverter structure. The expense of

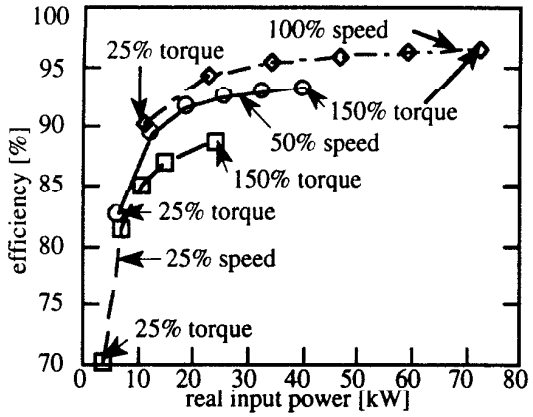

Fig. 16 Matrix converter efficiency versus the real input power for various torques and speeds (SKM400GA122D devices; T_j=125°C; f_s=10kHz).

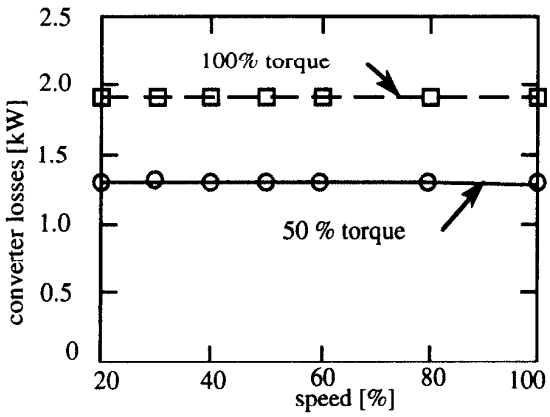

Fig. 17 Matrix converter losses versus the normalized speed for various torques (SKM400GA122D devices; T_j=125°C; f_s=10kHz).

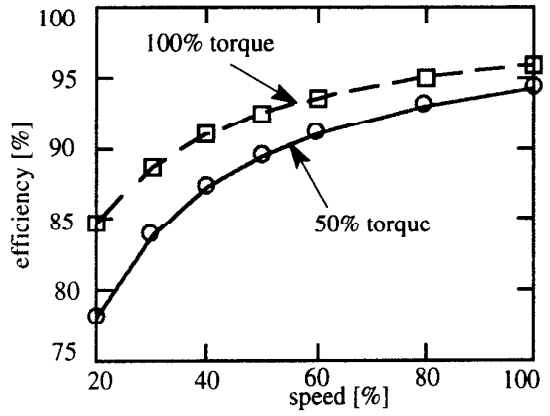

Fig. 18 Matrix converter efficiency versus the normalized speed for various torques (SKM400GA122D; T_j=125°C; f_s=10kHz).

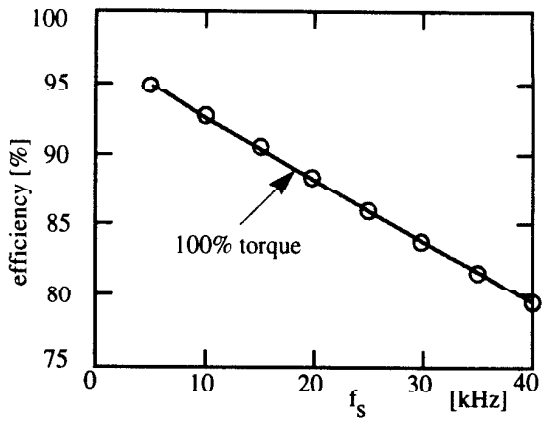

Fig. 19 Matrix converter efficiency versus the switching frequency (100% torque; 50% speed; SKM400GA122D devices; T_j=125°C).

semiconductors of a matrix converter would be even substantially lower if one would use reverse blocking NPT-IGBTs instead of the conventional common collector configuration [5].

VII. CONCLUSIONS

Technical issues concerning the application of matrix converters to field oriented induction motor drives have been described in this paper. A matrix converter switching sequence combination which minimizes harmonic components of the matrix converter input currents was described. It was demonstrated that small size capacitors work efficiently as input filters. It was verified that the required total power of the switches can be the same in both the matrix converter and a comparable dc-voltage-link converter. A further reduction of the installed total switch power of the matrix converter will be possible in the future when forward and reverse blocking NPT-IGBTs are available.

REFERENCES

[1] L. Gyugyi and B. R. Pelly, Static Power Frequency Changers. New York: Wiley-Interscience, 1976.

[2] A. Alesina and M. Venturini, "Solid state power conversion: A Fourier analysis approach to generalized transformer synthesis," IEEE Transactions on Circuit Systems, Vol. CAS-28, No. 4, 1981, pp. 319-330.

[3] A. Alesina and M. Venturini, "Analysis and design of optimum-amplitude nine-switch direct ac-ac converters," IEEE Trans. on Power Electronics, Vol. 4, No. 1, Jan. 1989, pp. 101-112.

[4] D.W. Novotny and T.A. Lipo, "Vector Control and Dynamics of AC Drives" , Oxford Press, 1996 (to appear).

[5] S. Bernet, T. Matsuo and T.A. Lipo, "A Matrix Converter Using Reverse Blocking NPT-IGBTs and Optimized Pulse Patterns", Conference Record IEEE-PESC, Baveno, Italy, June 24-27, 1996, to appear.

[6] T. Matsuo, S. Bernet and T.A. Lipo, "Modeling and Simulation of Matrix Converter/Induction Motor Drive", Conference Record IMACS'96, St. Nazaire, France, 1996.